

Non-Gaussian Diffusion Model for Phosphorus in Silicon Heavy-Doped Junctions

Frank Wirbeleit

GLOBALFOUNDRIES, 2070 Route 52, Hopewell Junction, NY 12533

Email: Frank.Wirbeleit@globalfoundries.com

Abstract

Besides common implant techniques, dopant diffusion enables steep diffusion profiles in heavily doped deep-source drain and ultra-shallow junctions as required in advanced microelectronic technology. Experimental phosphorus dopant diffusion profiles in silicon are described by a rational function diffusion (RFD) model, based on direct solution of Fick's equations and suitable for actual work in junction engineering.

Keywords: phosphorus, diffusion, junction, FET, device

Introduction

Heavily doped junctions of field effect transistor (FET) devices are key elements for controlling short channel effects (SCE) and junction resistance in aggressive pitch scaling at 32nm and beyond in advanced microelectronic technology [1]. Ultra-shallow junctions by phosphorus diffusion out of CVD film has been demonstrated [2]. By using heavy in situ doped epitaxial source drain contacts, retrograde dopant concentration profiles become much more achievable than with traditional heavy implant techniques [3,4]. Other work demonstrates that phosphorus is not only used in n-FET junction engineering, but also as co-dopant for boron diffusion control [5,6]. Heavy-doped junctions are sources of dopant diffusion in two directions with contradictory technological requirements. For the vertical direction (into the substrate), a sufficiently large diffusion length of dopants is required to bottom out the junction (especially in SOI technology) and to minimize the electrical source drain capacity load of FET; for the horizontal direction (towards the FET channel), to provide low extension and channel connectivity at a very short diffusion length for SCE control (threshold voltage roll off and scattering). Understanding and describing phosphorus diffusion profiles in simple models is therefore desired.

Experiments

Two samples of 5-inch mono-crystalline silicon wafers at a ground boron doping level corresponding to 20 Ohm cm^{-1} are set up by standard SC1, SC2 cleans for short- and long-time phosphorus diffusion processes. These samples were processed in furnaces with N₂ and vapor POCL₃ atmosphere at 750 °C/8 min. (short time exp.) and 900 °C/14 min. (long time exp.) under common clean conditions used in the semiconductor industry. After the experiments, the doping profiles of these samples are analyzed by high-resolution spreading resistance method (SRM) as shown in Fig.1. The near surface doping concentration of both samples results in very low sheet resistance. Because of the applied high-resolution SRM method, this very low surface sheet resistance could not be measured and a cut off in the near-surface high dopant concentration region is visible in the experimental data of Fig. 1. Phosphorus penetration profiles similar to Fig. 1 are also found in the literature [7]. The experimental error of SRM is estimated within a few percent in near-surface/high-concentration range and much less in mid- and low-concentration range because of non-activated phosphorus.

Discussion

As can be seen in Fig. 1, the Gaussian diffusion model is insufficient to predict the experimental detected phosphorus concentration profiles. In particular, the mismatch between the Gaussian diffusion model and the experimental data in the mid- and low- concentration range can not be predicted with the surface concentration at the same time (see Fig. 1). Different authors in the literature corrected the mismatch in mid and low concentration range by multiple superimposed Gaussian profiles [8, 9]. Otherwise, a similar mismatch as shown in Fig. 1 remains [7, 10-12].

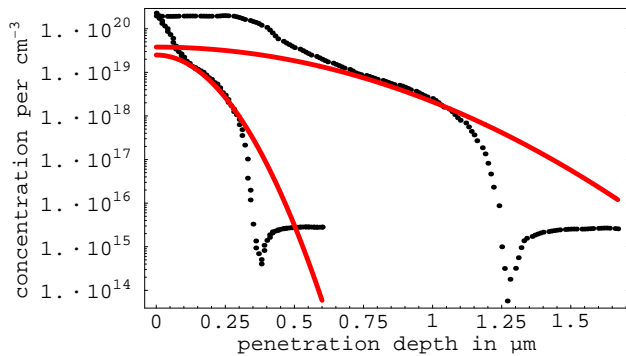


Figure 1: Doping concentration profiles of samples (dotted lines) and the approximated Gaussian distribution functions. Applied approximations are $2.5 \times 10^{19} \exp(-6x)^2$ and $3.8 \times 10^{19} \exp(-1.7x)^2$.

Partial Gaussian models are justified by different physical processes, for instance:

- impurity-vacancy effects (high-dopant concentration)
- different self-diffusion processes (effective diffusion coefficient)
- intrinsic diffusions (medium-dopant concentration)
- transient enhanced diffusion TED (low-dopant concentration, tail of doping profiles)
- abnormal phosphorus diffusion (low-concentration range)

Since diffusion theory is based on Fick's equations, analytical solutions besides the Gaussian function are analyzed first, before increasing model complexity. In this investigation, a certain direction x is applied (denoted as penetration depth) for simplification. The surrounding volume is taken as constant. These assumptions are denoted as a flat diffusion interface in the literature and are appropriate to the applied experimental conditions. Furthermore, a concentration-independent diffusion constant D is used for the same reason. The first of Fick's equations (Equ. 1.1) describes a change of concentration c per volume and is related to a mass

flow:

$$\frac{\partial m}{\partial t} + AD \frac{\partial c}{\partial x} = 0 \quad (1.1)$$

Fick's second equation (Equ. 1.2) describes a local concentration profile that is smoothed out over time. This equation assumes that no heat is produced during the diffusion process and no heat is accumulated in the solid (see also [13]), which is valid in the given experiments:

$$\frac{\partial c}{\partial t} = D \frac{\partial^2 c}{\partial x^2} \quad (1.2)$$

Taking into account that the mass per volume is defined as concentration c , Equ. 1.1 and 1.2 can be consolidated. The result is given in Equ. 1.3 and describes a snapshot of a diffusion profile as found in the experiments and also used in literature for generalized simulation of diffusion profiles [14].

$$\frac{\partial^2 c}{\partial x^2} + \frac{1}{x} \frac{\partial c}{\partial x} = 0 \quad (1.3)$$

Equ. 1.3 is still time-dependent, because the concentration oscillation term $\partial^2 c / \partial x^2$ translates into fluctuation in time $\partial c / \partial t$ (see Equ. 1.2) and the diffusion time t influences the diffusion length L , which becomes a parameter of solutions of Equ. 1.3 later on. All mathematical functions satisfying Equ. 1.1 – 1.3 are valid for describing diffusion and, besides the Gaussian function, there are obviously alternative mathematical solutions. Depending on certain experiments, one or more of these mathematical solutions can be selected and interpreted in terms of a physical model.

A. Alternative Diffusion Models

A solution of Equ. 1.3 is given by $\partial c / \partial x = a * 1 / x$ (a is a constant). This solution is a logarithmic function as given in Equ. 2.1 with additional constants for further discussion and called logarithmic function diffusion model (LFD model)

$$c = a * (b - \ln[e + x]) + d \quad (2.1)$$

Another solution of Equ. 1.3 is a quadratic term: $c = (a - x)^2 + d$. This term can be extended in the more general case of a rational function diffusion (RFD) model as given in Equ. 2.2:

$$c = a * z^n + d; \text{ with } z = \frac{b - x}{n - 1} \text{ for } n \neq 1 \quad (2.2)$$

Because of the cylindrical type of Equ. 1.3, Bessel functions $J_n(x)$ are mathematical solutions. By the special type of Equ. 1.3, the order n of the Bessel function is set to the same magnitude as x to satisfy the condition $n^2 / x^2 = 1$. Exploring this kind of Bessel function, n and x have the same sign; otherwise, the Bessel function would show a periodic behavior. In Equ. 2.3, additional constants are introduced as before, which gives the Bessel function diffusion (BFD) model:

$$c = a * (b + J_x[x]) + d \quad (2.3)$$

The slopes of mathematical functions in Eqs. 2.1 - 2.3 are adaptable to the physical expectations of a diffusion model in general, e.g., they predict a certain surface concentration and limited penetration depth of dopants. Hence, these functions have different slopes, singularities, and so on, which will make them more or less suitable to interpret given experimental data. All diffusion models will be examined to satisfy the following conditions:

- (i) At a penetration depth of zero, a surface concentration c_0 has to be predicted.
- (ii) The dopants concentration drops to zero at a maximum diffusion length L_0 . This maximum penetration depth is a clear defined value, smaller than infinite in most cases.

Condition (i) is commonly used. Condition (ii) is more restricted than commonly applied in the literature, in which a zero concentration of dopants is always expected at an infinite distance from the surface. Condition (ii) is not in contrast to that, but more specific. For describing different diffusion types/materials, the diffusion model can provide additional parameters not all set up in this work and focusing on phosphor diffusion in mono-crystalline silicon only.

B. Application of Alternative Diffusion Models

In Fig. 2.1, the logarithmic function of the LFD model (Equ. 2.1) is approximated to experimental data. The penetration depth x of Equ. 2.1 is given in relation to the maximum diffusion length L_0 . Condition (i) can be satisfied by interpreting the model parameter a of Equ. 2.1 as surface concentration c_0 . Boundary condition (ii) is satisfied clearly by the model function. A close surface peak indicates a singularity of the model at the surface interface, which can be improved by another model parameter set (e.g., $0.15 * [1 - \log(1 - x / 1.25 * 1.7)]$), or point to a segregation effect in physics. Using RFD model (Equ. 2.2), the best approximation of experimental data is obtained, as shown in Fig. 2.2. Only an edge close to the surface of the samples profiles in Fig. 2.2 indicates a second surface diffusion process, which is known as high-dose doping effect and will be discussed later. In order to satisfy the boundary conditions (i) and (ii), the parameter a of the RFD model is set to the surface concentration c_0 , b is set to one, and x is used in relation to the maximum diffusion length L_0 as before. The power n of the model was set to two and might change in the future. To approximate the experimental data by the BFD model as shown in Fig. 2.3, the parameter a of Equ. 2.3 is set to the surface concentration c_0 and the penetration depth x is given as $1-x/L_0$ according to the boundary conditions (i) and (ii). As shown in Fig. 2.3, the approximation result of the BFD model is similar to the LFD model approximation shown in Fig. 2.1, with a bigger mismatch at sample surface and at the tail of the concentration profiles. For this reason, the surface concentration c_0 and maximum diffusion length L_0 of this model are expected to be less accurate. A comparison of all model parameters' surface concentration c_0 and maximum diffusion length L_0 is given in Table 1.

Model	shallow profile		deep profile	
	c_0 [10^{19} cm^{-3}]	L_0 [μm]	c_0 [10^{19} cm^{-3}]	L_0 [μm]
Gauss	2.5	0.41	3.8	0.77
LFD	0.5	0.35	0.5	1.25
RFD	4	0.34	5	1.25
BFD	1	0.30	0.44	1.20

Table 1: Comparison of diffusion model parameters after approximation to experimental data shown in Fig. 1, 2.1-2.3:

According to Table 1, all alternative diffusion models predict a fairly matched maximum diffusion length L_0 . Depending on goodness of approximation at the shoulder of the diffusion profile slope, the surface concentration c_0 in Table 1 differs. The RFD model is in best agreement at dopant surface concentrations with the Gaussian model at both profiles, shallow and deep. In literature, the Gaussian model is used for predicting surface concentration ([15]), and therefore provides the reference c_0 in this comparison of all models (see Table 1). Because no Gaussian approximation of concentration profiles tail in low-concentration range is found in literature, the RFD and Gaussian model can not be compared in this regard. Simulated numerical diffusion profiles found in [16] are in agreement with this work, that experimental concentration profiles expose a stronger drop at the tail than the Gaussian model can predict.

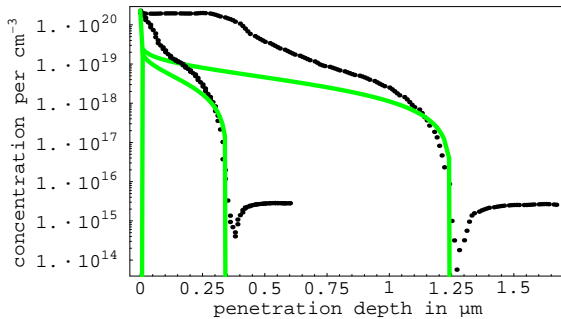


Figure. 2.1: Approximation of LFD model given in Equ. 2.1 (straight lines) to data (dotted lines) with the parameters $a=5 \times 10^{18} \text{cm}^{-3}$ (both profiles), $b=d=e=0$, $x_0 \rightarrow x/0.35 \mu\text{m}$ and $x_1 \rightarrow x/1.25 \mu\text{m}$ respectively.

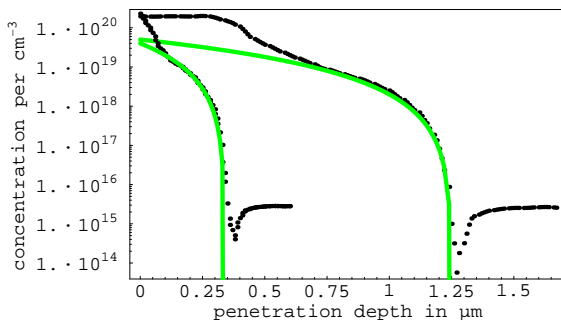


Figure 2.2: Approximation of RFD- model (straight lines) after Equ. 2.2 at experimentally detected diffusion profiles (dotted lines). The applied parameters for both profiles are $n=2$, $b=1$, $d=0$ and, for each profile separate $a=4 \times 10^{19} \text{cm}^{-3}$, $x_0 \rightarrow x/0.34 \mu\text{m}$ and $a=5 \times 10^{19} \text{cm}^{-3}$ for $x_1 \rightarrow x/1.25 \mu\text{m}$.

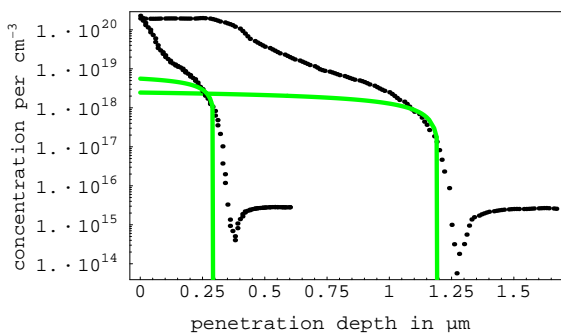


Figure 2.3: Approximation of BFD-model (straight lines) after Equ. 2.3 at two experimentally detected diffusion profiles (dotted lines). The following parameters are used: $a=10^{19} \text{cm}^{-3}$ and $a=0.44 \times 10^{19} \text{cm}^{-3}$, $b=1$, $d=0$, $x_0 \rightarrow 1-x/0.30 \mu\text{m}$ and $x_1 \rightarrow 1-x/1.20 \mu\text{m}$ respectively.

From literature, the Gaussian model is preferably applicable to the so-called volume diffusion processes close to the surface concentration, up to a concentration drop of about two orders of magnitude. In self-diffusion processes (mid-concentration range), the Gaussian model does not seem to be not adequate. Medium- and low-doping concentration range computer simulations of a kick-out diffusion process show dopant concentration profiles inadequate to the Gaussian model [11,12] also, but adequate to the RFD model. By other diffusion simulations [14], the presented analytical RFD model concentration slope seems to be confirmed for a low- and medium-dopant concentration, up to an upper limit of c_0 of around $1.5 \times 10^{19} \text{cm}^{-3}$ for phosphorus in silicon. In mid- and low-concentration range, the dopant diffusivity is almost linear to the dopant concentra-

tion. For heavy dopant concentrations ($1.5 \times 10^{19} \text{ cm}^{-3}$ for phosphorus), an additional surface diffusion mechanism kicks in (compare mismatch of RFD model in Fig. 2.2). In this concentration range, a vacancy mechanism contributes to an enhanced diffusivity, with phosphorus diffusivity proportional to the square of the concentration. A model of this diffusion mechanism can be introduced by superposition of a second model based on Fick's equations. Reviewing plots in Fig. 2.1-2.3, LFD and BFD model can represent a close surface doping profile better than the RFD with a power of two or the Gaussian model because of the strong drop in low-concentration range. In Fig. 3, a diffusion model based on the superposition of the RFD and LFD models is therefore shown.

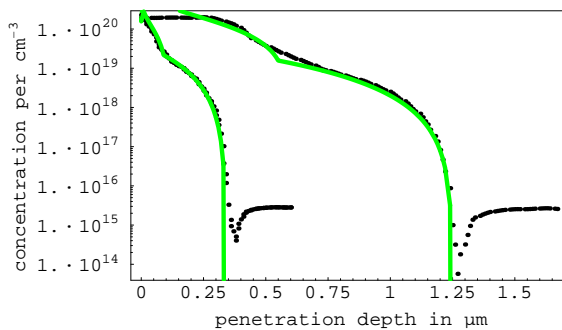


Figure 3: Approximation of experimental concentration profile (dotted lines) by superposition of RFD and LFD model (solid line). The following parameters are used. RFD model: $n=2$, $b=1$, $d=0$ and for each profile separately $a=4 \times 10^{19} \text{ cm}^{-3}$, $x \rightarrow x/0.34 \mu\text{m}$ and $a=5 \times 10^{19} \text{ cm}^{-3}$, $x \rightarrow x/1.25 \mu\text{m}$. LFD model: $b=d=e=0$, $a=1.1 \times 10^{20} \text{ cm}^{-3}$ and $a=2 \times 10^{20} \text{ cm}^{-3}$, $x \rightarrow x/0.09 \mu\text{m}$ and $x \rightarrow x/0.55 \mu\text{m}$.

Conclusion

Based on mathematical solutions of Fick's equations, different diffusion models can be taken into account. If an adequate approximation of experimental data can be obtained by a different solution of Fick's equations than the Gaussian function, it is worth taking this into consideration rather than increasing model complexity. Compared to recent diffusion simulation study of boron and phosphorus [17] with TSUPREM-4 software, a similar fit of experimental data was found as presented in this work. This might have an impact on the experimental interpretation of Gaussian-based diffusion models for transient enhanced diffusion (TED) [18].

Acknowledgement

I thank Mr. Karl-Heinz Stegemann for his support of this work.

References

- [1] Kang, Inkuk : "Formation Of N+P Junctions using In-Situ Phosphorus Doped Selective Si(1-X)Ge(X) Alloys..", theses 2004, Graduate Faculty of North Carolina State University, USA
- [2] Krüger, D.; Schlote, J.; et al. : "Shallow junction formation by phosphorus diffusion ..", *Microelectronic Engineering*, ISSN 0167-9317, 26(1995)2, pgs. 119-129
- [3] Yang, B.(Frank); Takalkar, R.; et al.: "High Performance nMOSFET with in-situ Phosphorus -doped embedded. Si:C..", *IEDM Conference 2008, Session 3.1, Tech. Digest*, pgs. 51-54
- [4] Ikutaa, Tetsuya; Fujitaa, Shigeru; Iwamoto, Hayato: "Characteristics of in-situ phosphorus-doped silicon ..", *Journal of Crystal Growth*, 310(2008)21 ,pgs. 4507-4510
- [5] Bae, Jicheul; Lee, Youngjae: "Excimer Laser-Assisted In Situ Phosphorus Doped SI(1-X)Ge(X) EPI Layer Activation", *ETRI Journal*, 25(2003) 4, pgs. 247-252
- [6] Hsieh, J.C.; Fang, Y.K.; et al.: "Characteristics of MOS capacitors of BF₂ or B implanted polysilicon gate with and without POCl₃ co-doped", *Electron Device Letters, IEEE*, 14(1993) 5, pgs. 222 - 224

- [7] Yoshida, M. : “Basic Condition for the pair Diffusion Model of Group V Impurities in Silicon”, DIMAT conf. 1992 Kyoto, Japan, Trans Tech Publ., ISBN 0-87849-662-9, pgs. 955-960
- [8] Klotsman,S.M.; et al.: “Volume Diffusion of 3d and 4d Impurities in Tungsten Single Crystals”, DIMAT conf. 1992 Kyoto, Japan, Trans Tech Publ., ISBN 0-87849-662-9, pgs. 735-740
- [9] Dao Khac, An: “ Computer Calculations of Enhanced Diffusivity and Effective Activation Energy from Measured Profiles on Impurities in Silicon”, DIMAT conference 2000 Paris, France, Scitec Publications Ltd. Switzerland, ISBN 3-908450-60-8, pgs. 653-658
- [10] Hood, G.M. : “Diffusion in Zr, HCP and open Metals”, DIMAT conf. 1992 Kyoto, Japan, Trans Tech Publ., ISBN 0-87849-662-9, pgs. 755-774
- [11] Stolwijk,N.A.: ”Atomic Transport in Semiconductors ...”, DIMAT conference 1992 Kyoto, Japan, Trans Tech Publ., ISBN 0-87849-662-9, pgs. 895-916
- [12] Pöpping, J.; Stolwijk,N.A.; Bösker, G.; Jäger, C.; Jäger, W.; Södervall, U.: “Measurements and Modeling of Zinc Diffusion Profiles in Gallium Phosphide”, DIMAT conf. 2000 Paris, France, Scitec Publ. Ltd. Switzerland, ISBN 3-908450-60-8, pgs. 723-730
- [13] Carslaw, H.S.; Jaeger, J.C. : “Conduction of Heat in Solids”, 2nd Ed. Oxford Univ. (1959), ISBN 0-19-853368-3
- [14] Uematsu, M.: “Unified Simulation of Diffusion in Silicon ..”, Defect and Diffusion Forum, 237-240 (2005) pgs. 38-49
- [15] Strohm,A.; Matics,S.; Frank,W.”Diffusion of Gold in Germanium”, DIMAT conf. 2000 Paris, France, Scitec Publications Ltd. Switzerland, ISBN 3-908450-60-8, pgs. 629-634
- [16] Dao Khac, An; Vu Ba, Dung: “Preliminary Results of Numerical Profiles for the Simultaneous Diffusion of Boron and Point Defects in Silicon using Irreversible Thermodynamic Theory”, DIMAT conference 2000 Paris, France, Scitec Publications Ltd. Switzerland, ISBN 3-908450-60-8, pgs. 647-652
- [17] Arai, E.; Iida,D.; Asai,H.; et al.: “Applicability of Phosphorus and Boron Diffusion Parameters..”, Jpn. J. Appl. Phys. 42(2003)1, No.4A, pgs. 1503
- [18] Jain,S.C.; Schoenmaker,W.; Lindsay,R.;et al.:”Transient Enhanced Diffusion of Boron in Si”, J. Appl. Phys., 91(2002)11, pgs. 8919-8941